BAH domains and a histone-like motif in DNA methyltransferase 1 (DNMT1) regulate *de novo* and maintenance methylation *in vivo*

Received for publication, June 25, 2018, and in revised form, October 12, 2018 Published, Papers in Press, October 19, 2018, DOI 10.1074/jbc.RA118.004612

Olya Yarychkivska[‡], Zoha Shahabuddin[‡], Nicole Comfort[§], Mathieu Boulard[¶], and Timothy H. Bestor[‡1]

From the Departments of [‡]Genetics and Development and [§]Environmental Health Science, College of Physicians and Surgeons of Columbia University, New York, New York 10032, and [¶]European Molecular Biology Laboratory, 00015 Rome, Italy

Edited by Eric R. Fearon

DNA methyltransferase 1 (DNMT1) is a multidomain protein believed to be involved only in the passive transmission of genomic methylation patterns via maintenance methylation. The mechanisms that regulate DNMT1 activity and targeting are complex and poorly understood. We used embryonic stem (ES) cells to investigate the function of the uncharacterized bromo-adjacent homology (BAH) domains and the glycine–lysine (GK) repeats that join the regulatory and catalytic domains of DNMT1. We removed the BAH domains by means of a CRISPR/Cas9-mediated deletion within the endogenous *Dnmt1* locus. The internally deleted protein failed to associate with replication foci during S phase *in vivo* and lost the ability to mediate maintenance methylation. The data indicate that ablation of the BAH domains causes DNMT1 to be excluded from replication foci even in the presence of the replication focus–targeting sequence (RFTS). The GK repeats resemble the N-terminal tails of histones H2A and H4 and are normally acetylated. Substitution of lysines within the GK repeats with arginines to prevent acetylation did not alter the maintenance activity of DNMT1 but unexpectedly activated *de novo* methylation of paternal imprinting control regions (ICRs) in mouse ES cells; maternal ICRs remained unmethylated. We propose a model under which DNMT1 deposits paternal imprints in male germ cells in an acetylation-dependent manner. These data reveal that DNMT1 responds to multiple regulatory inputs that control its localization as well as its activity and is not purely a maintenance methyltransferase but can participate in the *de novo* methylation of a small but essential compartment of the genome.

DNMT1[2] is required for the maintenance of genomic methylation patterns during S phase (Ref. 1); for reviews, see Refs. 2 and 3). In biochemical assays, DNMT1 has a modest (<10-fold) preference for hemimethylated DNA (4) and has been assigned a function limited to maintenance methylation, although a role for DNMT1 in *de novo* methylation has not been excluded. Multiple mechanisms increase the fidelity of maintenance methylation; these include autoinhibition of *de novo* methylation by the C*XX*C domain (5) and the replication focus–targeting sequence (RFTS) (6), which can inhibit *de novo* methylation by occlusion of the active site of DNMT1 (7). The ubiquitin-like with PHD and Ring finger domains 1 (UHRF1) protein, which is required for faithful maintenance methylation *in vivo* (8, 9), recognizes hemimethylated CpG sites generated during DNA replication via its SRA domain (10–12). While bound to hemimethylated sites, UHRF1 recognizes nearby histone H3 methylated at lysine 9 with its TTD-PHD domains (13, 14) and ubiquitylates H3 at lysines 18 and 23, which is then bound by the RFTS domain of DNMT1 (15, 16). Binding of RFTS to ubiquitylated histone H3 brings about a conformational change in DNMT1, which increases its catalytic activity *in vitro* (17). UHRF1-dependent histone modifications have been proposed to affect maintenance methylation through effects on the interaction of DNMT1 with chromatin (15–17).

There has been a focus on the mechanism of interaction of UHRF1 and DNMT1, but little attention has been directed to the function of well-conserved domains located within the N-terminal regulatory region of DNMT1 that are not known to interact with UHRF1. Two bromo-adjacent homology (BAH) domains of unknown function are conserved among nearly all DNMT1 homologs. BAH domains are present in ~20 mammalian proteins of diverse function. Some BAH domains have been reported to bind to histone tails in a modification-dependent manner (for a review, see Ref. 18). BAH domains fall into two general groups: ORC1-like and SIR3-like. In DNMT1, BAH1 is a member of the ORC1-like group, and BAH2 is a member of the SIR3-like group. Just C-terminal of BAH2, a stretch of alternating lysine and glycine residues (the GK repeats) joins the N-terminal regulatory region and the C-terminal catalytic domain (19) and had been proposed to mediate the degradation of DNMT1 via an acetylation-dependent association with USP7 (20), but recent data indicate that the stability of DNMT1 is independent of the GK repeats and of USP7 (21).

This work was supported by National Institutes of Health Grant 5R21 HG009187 (to T. H. B.). The authors declare that they have no conflicts of interest with the contents of this article. The content is solely the responsibility of the authors and does not necessarily represent the official views of the National Institutes of Health.

[1] To whom correspondence should be addressed: Dept. of Genetics and Development, College of Physicians and Surgeons of Columbia University, 701 W. 168t St., New York, NY 10032. Tel.: 212-305-5331; E-mail: THB12@cumc.columbia.edu.

[2] The abbreviations used are: DNMT1, DNA methyltransferase 1; ES, embryonic stem; BAH, bromo-adjacent homology; RFTS, replication focus–targeting sequence; LUMA, luminometric methylation assay; ICR, imprinting control region; gRNA, guide RNA; UHRF1, ubiquitin-like with PHD and Ring finger domains 1; PHD, plant homeodomain; SRA, SET and Ring finger–associated domain; TTD, tandem Tudor domain; TRD, target recognition domain; IAP, intracisternal A-particle; PCNA, proliferating cell nuclear antigen.

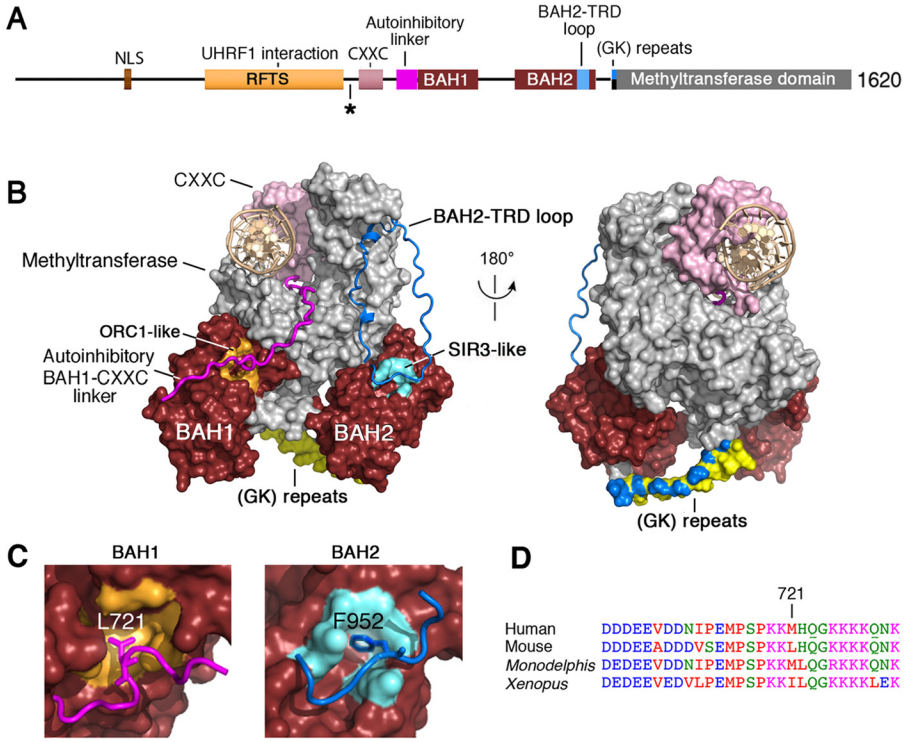

Figure 1. Domain organization and structure of DNMT1. *A*, functional domains of DNMT1: nuclear localization sequence (*NLS*) and RFTS (both from Ref. 6); *CXXC* domain, a zinc-binding motif that specifically binds to unmethylated CpG dinucleotides in DNA (for a review, see Ref. 52); BAH1 and BAH2 (for a review, see Ref. 18); GK repeats, a stretch of alternating glycine and lysine residues (19); and the methyltransferase domain, the catalytic domain with strong similarities to DNA (cytosine-5)-methyltransferases of prokaryotes and eukaryotes (for a review, see Ref. 2). *B*, crystal structure of DNMT1 in complex with unmethylated DNA (5). Sequences N-terminal of the *asterisk* in *A* have been omitted. The spatial relationship of the functional domains shown in *A* are depicted by means of a shared color scheme. The GK repeats were not structured in any of the crystal structures of DNMT1; therefore, their position is approximate. *C*, mode of binding of the autoinhibitory linker via a leucine residue to BAH1 (*left*) and binding of the BAH2-TRD loop via a phenylalanine (*right*). *D*, conservation of the BAH1-*CXXC* linker sequence among vertebrates.

We have addressed the function of the BAH domains and the GK repeats. We found that the BAH domains are required for maintenance methylation by mediating the association of DNMT1 with replication foci during S phase. Substitution of the GK repeats with GR repeats did not affect DNMT1 protein stability and did not affect maintenance methylation *in vivo*. It was very surprising to find that the GR substitution caused *de novo* methylation specifically of imprinting control regions (ICRs) in mouse embryonic stem (ES) cells that are normally methylated in male germ cells; maternal ICRs remained unmethylated. These and other data suggest that DNMT1 is likely to be involved in the *de novo* methylation of paternal ICRs in male germ cells.

Results

The BAH domains are necessary for targeting DNMT1 to replication foci during S phase

As shown in Fig. 1*A*, DNMT1 contains multiple functional domains. In the crystal structure of DNMT1 bound to unmethylated DNA (5) (Fig. 1*B*), the BAH domains are remote from the active site of the catalytic domain, but an acidic autoinhibitory linker extends from BAH1 to the *CXXC* domain, which binds to unmethylated CpG dinucleotides and prevents their entry into the active site of the catalytic domain (5). BAH2 extends a long solvent-exposed loop (the BAH2-TRD loop) that interacts with the target recognition domain (TRD) within the catalytic domain. The function of this interaction is unknown. Both the BAH1 autoinhibitory linker and the BAH2-TRD loops bind to the BAH-binding pockets (Fig. 1*C*) that in other proteins interact with histone tails in a manner that depends on the modification status of lysine residues (for a review, see Ref. 18). In the case of DNMT1, BAH1 binds to a sequence centered on Leu-721, whereas BAH2 binds to Phe-952; lysines are not involved in either case. However, interaction with neighboring lysines cannot be excluded as the BAH1-*CXXC* linker shifts positions between different conformations of DNMT1 (5, 22). The BAH1-*CXXC* linker is highly conserved among vertebrates (Fig. 1*D*).

To address the functions of the BAH domains, the endogenous *Dnmt1* locus was modified by Cas9-mediated deletion of exons 11–16 (Fig. 2*A*), which encode only the BAH domains and leave the remainder of the protein intact. The joining of exons 10 and 17 produces an in-frame splicing event. As shown in Fig. 2*B*, the DNMT1 protein lacking the BAH domains is stable and produced at levels very similar to that of the full-length protein. Internally deleted protein does not aggregate in the cytoplasm and localizes to the nucleus as does full-length DNMT1 (Fig. 2*C*). Two ES cell clones that had undergone homozygous deletions were subjected to further study.

DNMT1 is present at constant levels in populations of dividing cells but is recruited to replication foci at S phase (6). As shown in Fig. 2*C*, deletion of the BAH domains caused a failure of DNMT1 to be incorporated into replication foci with >90% of S-phase cells displaying a diffuse nucleoplasmic localization

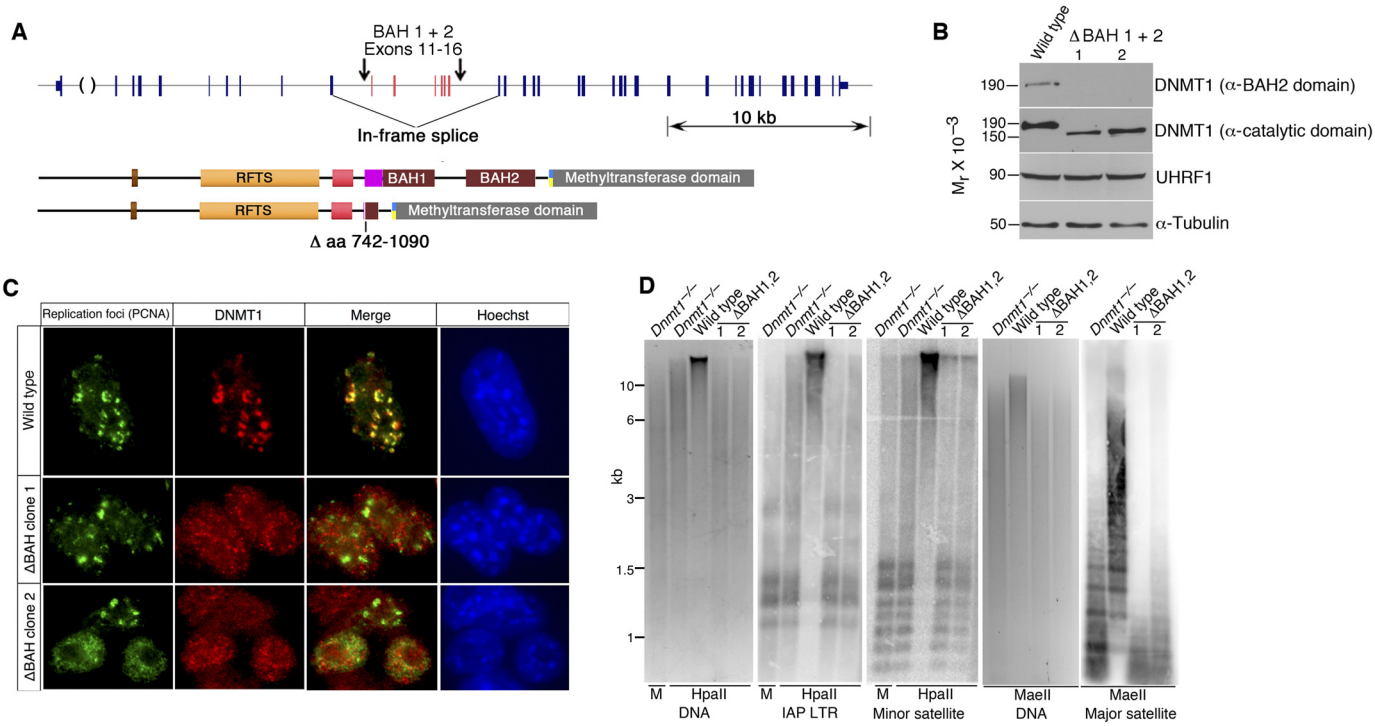

Figure 2. *In vivo* deletion of BAH domains eliminates DNA methylation and recruitment of DNMT1 to replication foci. *A*, Cas9-mediated deletion of exons encoding the BAH domains. Flanking exons undergo an in-frame splicing event; internally deleted protein product is shown below. *B*, immunoblot analysis shows that BAH domain deletions are stable and expressed at close to WT levels. Two independent clones are shown. *C*, failure of BAH deletion proteins to associate with replication foci. The *top row* shows that WT DNMT1 colocalizes with PCNA, a marker of replication foci, whereas the *bottom two rows* show that BAH-deleted DNMT1 fails to associate with replication foci. *D*, BAH-deleted DNMT1 fails to maintain genomic methylation patterns. In all cases, resistance to methylation-sensitive restriction enzymes (HpaII and MaeII) is equivalent between *Dnmt1*$^{-/-}$ ES cells and DNMT1 BAH-deleted ES cells. *aa*, amino acids; *LTR*, long terminal repeat.

in independent clones. This was unexpected as the RFTS is intact in the internally deleted protein, and recruitment of DNMT1 to replication foci had been reported to involve binding of the RFTS domain to histone H3 ubiquitylated by UHRF1 (16, 17). In addition, the isolated RFTS domain is capable of localizing to replication foci (6). The diffuse nucleoplasmic localization phenotype observed in cells with the BAH deletion is similar to that of *Uhrf1*-null ES cells (23). These data indicate that BAH domains are required for targeting of DNMT1 to replication foci during S phase even in the presence of the RFTS and UHRF1.

As shown in Fig. 2*D*, the BAH-deleted form of DNMT1 was unable to maintain DNA methylation genome-wide or at IAP retrotransposons and major satellite DNA, sequences that are normally densely methylated. Minor satellite DNA was partially methylated (Fig. 2*D*), which confirms that BAH-deleted DNMT1 has enzymatic activity *in vivo*. The inability of BAH-deleted DNMT1 to perform maintenance methylation is consistent with the failure of the protein to be incorporated into replication foci.

GK repeats are dispensable for maintenance DNA methylation

All known DNMT1 homologs contain at least one GK dipeptide between the N-terminal regulatory region and the C-terminal catalytic domain (Fig. 3*A*) (21). DIM-2, a DNMT1 homolog from the ascomycete *Neurospora crassa*, has a single GK dipeptide at this position (24). DNMT1 homologs of eutherian mammals contain 13 alternating Gly and Lys residues. The GK repeats are not resolved in any of the extant DNMT1 crystal structures and are likely to be very mobile; they are rendered in Fig. 1*B* to show the approximate spatial relationship of the GK repeats to the other domains of DNMT1. The GK repeats resemble the N-terminal tails of histones H2A and H4, which are also highly flexible. It had been previously shown that the GK repeats were not required for the stabilization of DNMT1 protein (21). The GK repeats are subject to acetylation at multiple lysine residues (25). We tested the function of the GK repeats by replacement of each of the lysines with arginine, which maintains the basic nature of the sequence but prevents acetylation.

Full-length DNMT1 bearing the GK → GR substitutions (Fig. 3*B*) was expressed in transfected *Dnmt1*$^{-/-}$ ES cells (26) under the control of the *Dnmt1* promoter, which causes DNMT1 to be expressed at close to the levels of endogenous DNMT1 (27). As shown in Fig. 3*C*, ES cell clones were obtained that expressed GR DNMT1 at levels very close to that of endogenous DNMT1. Levels of DNA methylation in cells expressing GR DNMT1 were compared with those of WT cells and *Dnmt1*$^{-/-}$ cells expressing recombinant GK DNMT1 of WT sequence. In contrast to the BAH deletion mutants, the GR mutants were capable of rescuing and maintaining DNA methylation genome-wide as assessed by luminometric methylation assay (LUMA) (Fig. 3*E*) and at IAP retrotransposons and minor satellite DNA (Fig. 3*D*). These data indicate that the GK repeats are not essential for the genome-wide maintenance of DNA methylation.

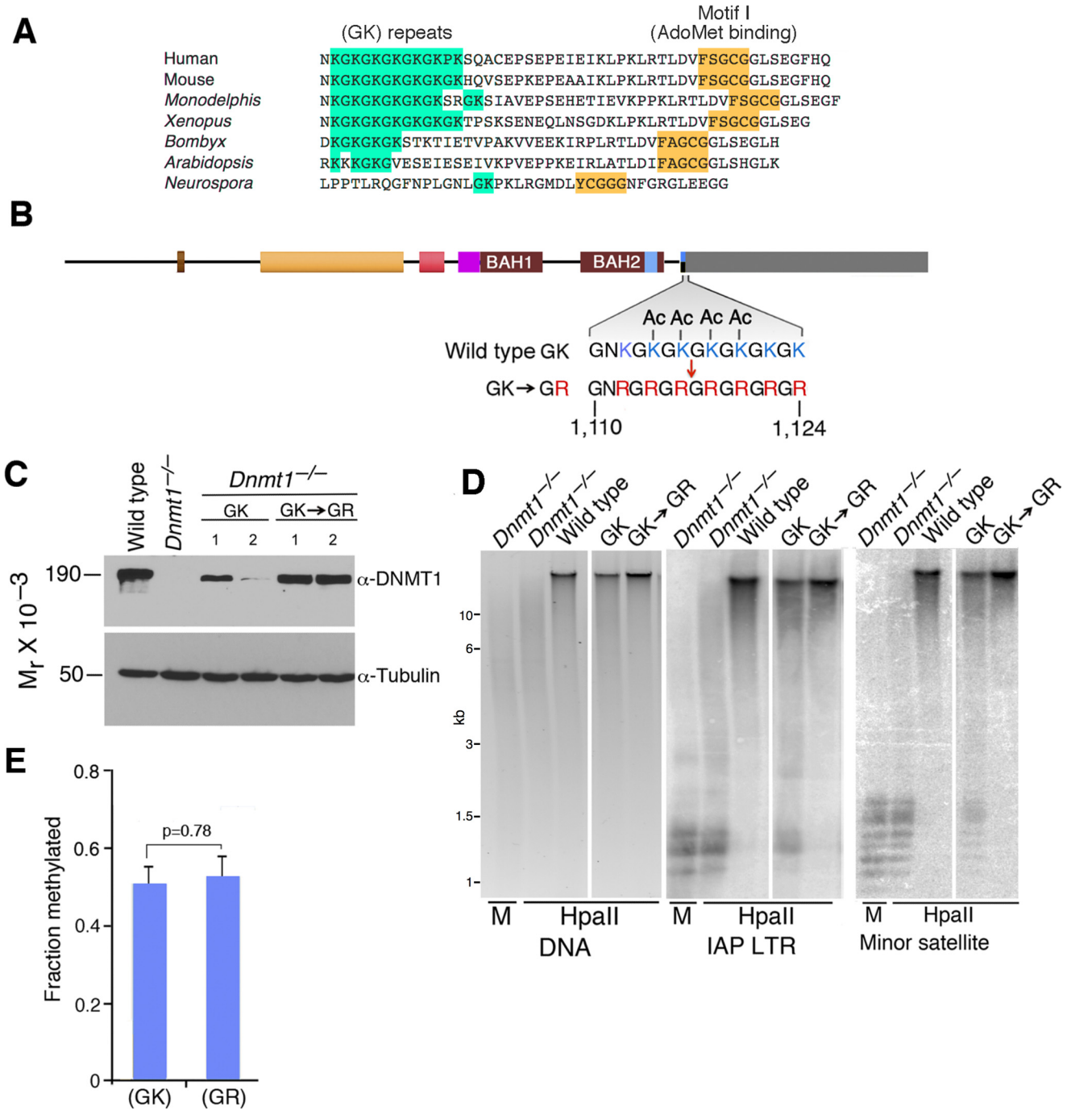

Figure 3. GK repeats are dispensable for maintenance methylation. GK DNMT1 or GR DNMT1 expression constructs were transfected into *Dnmt1*$^{-/-}$ ES cells and tested for restoration of genome-wide DNA methylation. *A*, conservation of GK repeats in DNMT1 homologs from animals, plants, and fungi. *B*, depiction of sequence change in GR DNMT1. *C*, immunoblot analysis that shows near WT levels of expression of GR DNMT1. *D*, restoration of WT levels of DNA methylation globally, at IAP long terminal repeat (*LTR*), and at minor satellites as established by measurement of resistance to methylation-sensitive restriction endonucleases and Southern blotting. *E*, quantification of genomic methylation levels by LUMA. *Error bars* represent S.D.

De novo methylation of paternal ICRs in the presence of GR DNMT1 but not GK DNMT1

As was shown in Fig. 3*D*, both GR DNMT1 and GK DNMT1 were capable of restoring genome-wide DNA methylation when expressed in *Dnmt1*$^{-/-}$ ES cells. *Dnmt1*$^{-/-}$ ES cells expressing either GR DNMT1 or GK DNMT1 were examined by bisulfite genomic sequencing for methylation at ICRs where allele-specific methylation confers allele-specific expression to imprinted genes (28–30). We analyzed methylation of all known paternally methylated ICRs, *H19*, *Dlk1*/*Gtl2*, and *Rasgrf1*, and the following maternal ICRs: *Igf2*, *Snrpn*, *Peg3*, *Kcnq1ot1*, and *Peg1*. It had previously been reported that *Dnmt1* rescue resulted in global genome remethylation, but allele-specific methylation at imprinted genes was not reestablished without passage through the germ line (31, 32). In accordance with these data, *Dnmt1*$^{-/-}$ ES cells that expressed GK DNMT1 showed full rescue of genome-wide DNA methylation but did not remethylate maternal or paternal ICRs. Sur-

prisingly, in the presence of GR DNMT1, all paternally methylated ICRs (*H19*, *Dlk1*/*Gtl2*, and *Rasgrf1*) underwent *de novo* methylation, whereas maternal DMRs (*Igf2*, *Snrpn*, *Peg3*, *Kcnq1ot1*, and *Peg1*) remained unmethylated (Fig. 4). Paternal ICRs exhibited a statistically significant gain of methylation in GR as compared with GK cells (Fig. 4*C*). We performed bisulfite sequencing of ICRs in biological replicates, demonstrating reproducibility of *de novo* methylation at paternal ICRs. These data indicate that lysine-to-arginine substitution that prevents acetylation of the GK repeats activates *de novo* methylation specifically at paternal ICRs.

Discussion

The preference of DNMT1 for hemimethylated DNA could have been predicted to result simply from the selective recognition and methylation of hemimethylated DNA. However, there is no evidence that this occurs, and DNMT1 does not possess a domain that is able to recognize and bind hemimethylated DNA. DNMT1 has a C*XX*C domain that binds unmethylated DNA and is involved in autoinhibition (5). In our study, we discovered that the BAH domains and the GK repeats are involved in two distinct targeting mechanisms, one to maintain DNA methylation in the case of BAH domains and one to carry out a novel function, *de novo* methylation of paternal imprints, in the case of the GK repeats.

The function of the two BAH domains of DNMT1 had not been previously addressed. We used a novel Cas9-mediated approach to delete the exons that encode the BAH domains from the endogenous *Dnmt1* locus. The internally deleted protein was stable and expressed at the same level as the full-length protein. However, it was unable to associate with replication foci during S phase and displayed a diffuse nucleoplasmic localization. The same localization phenotype has been observed in *Uhrf1*-null ES cells (23). Previous data had shown that the RFTS alone is capable of targeting heterologous proteins to replication foci (6). Based on these data, we conclude that in the absence of the BAH domains DNMT1 is actively excluded from replication foci by a mechanism that regulates conformational change within the molecule necessary for RFTS- and UHRF1-dependent targeting. We propose that this conformational change could be brought about by the autoinhibitory (BAH1-C*XX*C) linker, which forms hydrogen bonds with RFTS (22) and BAH1.

The function of the GK repeats was also unknown; a role in an acetylation-dependent interaction with USP7 that protected DNMT1 from proteasomal degradation (20) is unlikely to occur as the stability of DNMT1 is independent both of USP7 and of acetylation of the GK repeats (21). We addressed the function of the GK repeats by *in vivo* expression of a form of DNMT1 in which the GK repeats had been replaced by GR repeats, which maintains the basic nature of the sequence but prevents acetylation. GR DNMT1 was capable of restoring genome-wide methylation to the same extent as WT GK DNMT1, but GR DNMT1 also induced the *de novo* methylation of paternally methylated ICRs as observed in male germ cells. This surprising finding is supported by additional lines of evidence. First, the establishment of paternal genomic imprints is largely independent of DNMT3L (33) and of DNMT3A (34), whereas the establishment of maternal genomic imprints is completely dependent on DNMT3L (29) and DNMT3A (34). Second, although DNMT1 is not normally present in nondividing cell types, it is present in nondividing prospermatogonia (35) at the time when paternal genomic imprints are established (36). These data indicate that DNMT1 may carry out the *de novo* methylation of paternal ICRs and that regulated deacetylation of the GK repeats may target DNMT1 to these sequences in prospermatogonia. As has been noted previously, there is profound sexual dimorphism in genomic imprinting in mammals (37). Paternal ICRs are characterized by sequence characteristics distinctly different from those of maternal ICRs, and maternal ICRs are usually located at promoter regions, whereas paternal ICRs are found in intergenic regions and are not associated with promoters or known enhancers (38).

A role for DNMT1 in *de novo* methylation has never been excluded, although the enzyme has commonly been attributed a role strictly limited to maintenance methylation. This is largely due to the influence of predictions of the existence of an enzyme having this activity made in 1975 by Holliday and Pugh (39) and by Riggs (40). In fact, DNMT1 has a much higher specific activity on unmethylated DNA than either DNMT3A or DNMT3B in biochemical assays (41). Furthermore, DNMT1 is the only DNA methyltransferase homolog present in several insect orders that have methylated genomes (42). The methylated genome of the lepidopteran *Bombyx mori* encodes only a DNMT1 protein that is very similar to that of mammals and that according to the Conserved Domain Database (43) contains no conserved domains not also present in mammalian DNMT1 (Fig. 5). This suggests that DNMT1 must be involved in both *de novo* and maintenance methylation in *Bombyx*. We speculate that in mammalian spermatogonia one or more factors selectively recognize and bind to unmethylated paternal ICRs; these factors recruit and deacetylate the GK repeats of DNMT1 to activate the *de novo* activity of DNMT1 specifically at paternal ICRs.

These results show that DNMT1 is not a simple enzyme that recognizes and methylates hemimethylated CpG dinucleotides immediately after passage of the replication fork. It is instead under multiple regulatory inputs and may play a much larger role in the dynamics of genomic methylation patterns than may have been formerly believed.

Experimental procedures

Cell culture

Mouse ES cells were cultured on gelatin at 37 °C with 5% CO_2 in Dulbecco's modified Eagle's medium supplemented with 15% fetal bovine serum, 2 mM L-glutamine, minimum essential medium nonessential amino acids, 100 IU/ml penicillin, 100 μg/ml streptomycin, 0.12 mM 2-mercaptoethanol, and leukemia inhibitory factor from the conditioned medium of leukemia inhibitory factor–secreting cells.

Generation of rescue ES cell lines

Stable ES cell lines were generated by nucleofection of 2×10^6 *Dnmt1*-null ES cells (26) with 19 μg of MT80 minigene (27) and 1 μg of PGKPuro plasmid (for puromycin resistance) using

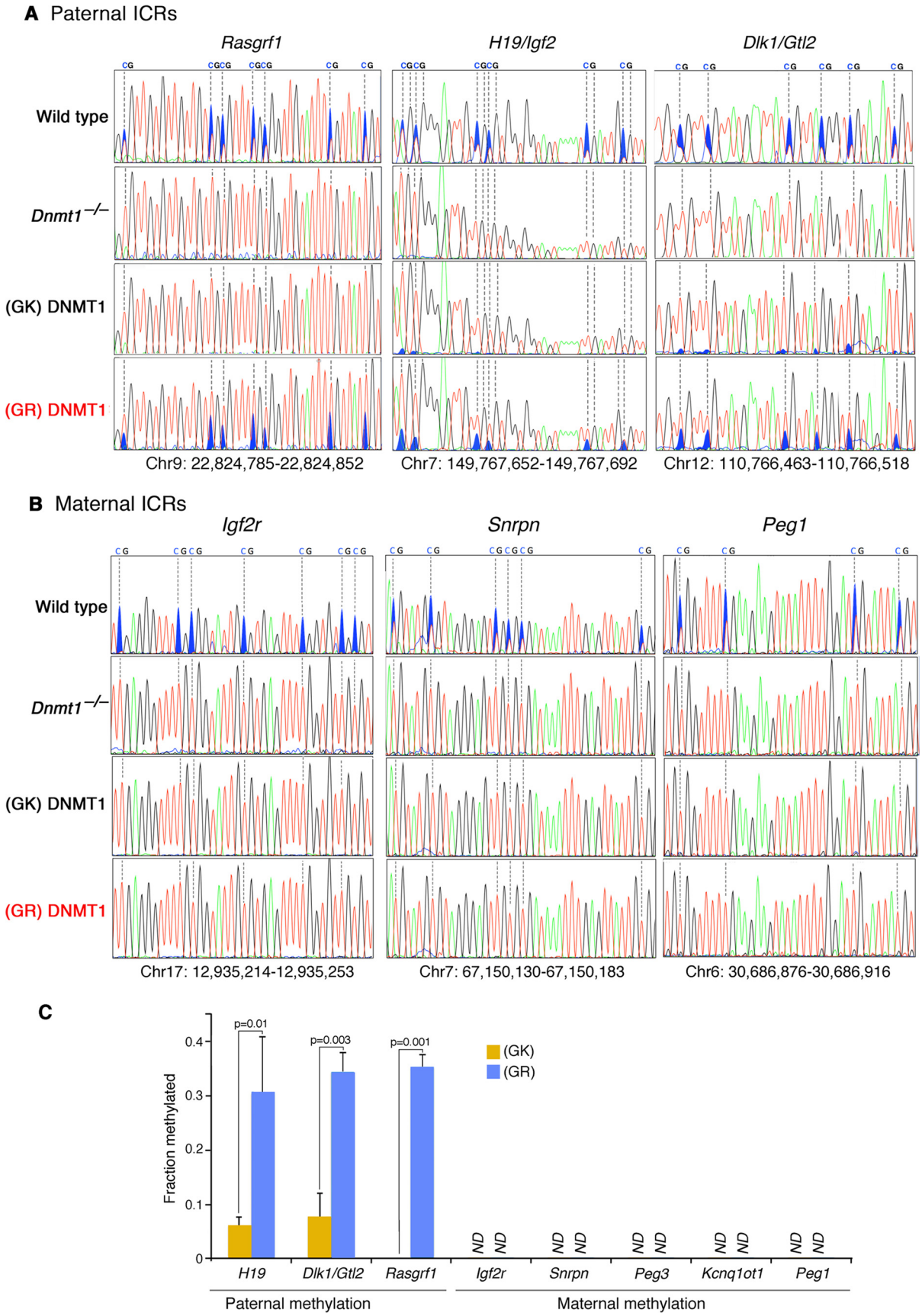

Figure 4. Specific *de novo* methylation of paternal ICRs by GR DNMT1. The GK DNMT1 and GR DNMT1 ES cell clones shown in Fig. 3 were examined for DNA methylation by bisulfite genomic sequencing at paternal ICRs (*A*) and maternal ICRs (*B*). Positions of CpG dinucleotides are shown by *dotted lines*. *C* shows that *de novo* methylation at paternal ICRs was much greater in the presence of GR DNMT1. *Chr*, chromosome; *ND*, not detected. *Error bars* represent S.D.

In vivo regulation of DNMT1

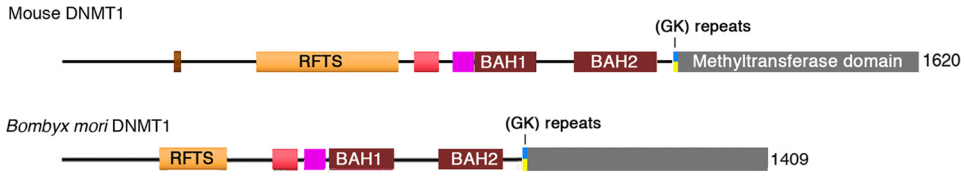

Figure 5. Functional domains in mouse and *B. mori* homologs of DNMT1. DNMT1 is the only DNA (cytosine-5)-methyltransferase homolog detected in the *Bombyx* genome (42) but does not contain any annotated domains not also present in mammalian DNMT1 as assessed by CDD/SPARCLE (43). This indicates that DNMT1 is very likely to be involved in both maintenance and *de novo* methylation in *Bombyx* and suggests that the same is likely to be true of mammalian DNMT1.

Amaxa P3 Primary Cell 4D-Nucleofector X Kit L. Nucleofected cells were seeded onto mouse embryonic fibroblast extracellular matrix in 15-cm dishes. MT80 minigene, carrying 12 kb of 5′ *Dnmt1* genomic sequence with endogenous promoter and 5.5 kb of *Dnmt1* cDNA (27), was modified by the addition of an N-terminal FLAG-HA tag after the translation start site. Mutations were introduced using the QuikChange Site-Directed Mutagenesis kit (Agilent). Individual clones were selected with puromycin (2 μg/ml) for 10–14 days and picked into 96-well plates. Clones were genotyped using primers specific to the FLAG-HA tag and *Dnmt1* (forward primer, GGACTACAAGGACGACG; reverse primer, GCTGACCAAAGAGGGGAACC). Positive clones were propagated, and levels of DNMT1 expression were tested by immunoblotting. Clones expressing DNMT1 at WT levels were selected for further studies.

Generation of CRISPR/Cas9 ES cell lines

To delete BAH domains, Broad Institute software was used to design gRNAs targeting introns upstream of BAH1 and downstream of BAH2 of endogenous *Dnmt1* locus (Table 1). gRNAs were cloned into pX330-PURO plasmid. 5–10 μg of plasmid DNA was nucleofected into 2 million WT CCE mouse ES cells (derived from 129/Sv mouse strain) (44, 45) using Amaxa P3 Primary Cell 4D-Nucleofector X Kit L. Nucleofected cells were seeded onto mouse embryonic fibroblast extracellular matrix in 15-cm dishes. Transient selection with puromycin (1 μg/ml) was applied 48 h postnucleofection for a period of 24 h. Surviving clones were picked 10–14 days after nucleofection. Remaining clones were pulled for genomic DNA and tested with T7 endonuclease to check the percentage of cuts in the population. Individual clones were genotyped using primers flanking the deletion site (forward primer, CAGGTAGCCCATCCGCTTG; reverse primer, AATTCCTAGCACCCACACGG; expected product size, 333 bp). Homozygous and heterozygous clones were distinguished by using one primer outside the deleted site and one primer inside (forward primer, CAGGTAGCCCATCCGCTTG; reverse primer, CAGTAAGATCCCATCTCCAAACCA; expected product size, 291 bp for WT allele and no product for deleted allele).

Immunoblotting

Whole-cell extracts were prepared by lysis in radioimmune precipitation assay buffer (150 mM NaCl, 1% Nonidet P-40, 0.5% deoxycholic acid, 0.1% SDS, 50 mM Tris, pH 7.5), briefly sonicated to disrupt genomic DNA, then heated to 100 °C in SDS, and loaded for SDS-PAGE. Proteins were transferred to nitrocellulose membrane and blocked in 5% milk, 0.1% Tween 20, PBS for 1 h at room temperature. Blots were incubated at 4 °C overnight with primary antibodies in 10% fetal bovine serum, 0.1% Tween 20. After incubation with DNMT1 antibody, blots were washed with PBS with 0.1% Tween 20 and with PBS. The following antibodies were used: rabbit polyclonal to DNMT1 (Cell Signaling Technology, 5032 (D63A6); 1:2500 dilution), mouse monoclonal to DNMT1 (Santa Cruz Biotechnology, sc-271729; 1:1000), rabbit polyclonal to HA tag (Abcam, Cambridge, UK, ab9110; 1:5000), and mouse monoclonal to α-tubulin (Abcam, ab7291; 1:10,000).

Methylation analysis

Genomic DNA was extracted by digestion with proteinase K and RNase A followed by phenol/chloroform extraction and isopropanol precipitation. Genomic DNA was digested for two rounds with methylation-sensitive enzyme HpaII, its isoschizomer MspI as a control, or MaeII (for major satellite analysis). All enzymes were from New England Biolabs. DNA was quantified, fractionated on 0.8% agarose gels, and stained with ethidium bromide.

Southern blot analysis was performed with IAP probes generated by PCR (forward primer, GGTAAACAAATAATCTGCGC; reverse primer, CTGGTAATGGGCTGCTTCTTCC). DNA in agarose gels was transferred to a Nytran SuPerCharge (SPC) membrane (GE Healthcare) overnight in 10× SSPE buffer (1.5 M sodium chloride, 0.1 M sodium phosphate, 0.01 M EDTA, pH 7.4). After cross-linking, membrane was prehybridized with 6× SSC, 5× Denhardt's, 1% SDS, 10% dextran sulfate for 1 h at 45 °C and incubated overnight with IAP probe at 45 °C. Membranes were washed once with 2× SSC, 0.5% SDS; twice with 1× SSC, 0.5% SDS; and once with 0.2× SSC, 0.5% SDS.

Global levels of DNA methylation were quantified using LUMA as described previously (46). 400 ng of genomic DNA was digested with MspI/EcoRI and HpaII/EcoRI in parallel. The overhangs from the enzymatic digestion were quantified by pyrosequencing (PyroMark Q24, Qiagen, Hilden, Germany) with the following dispensation order: GTCACAGTGT. Global DNA methylation levels were calculated from the peak heights at positions 3, 4, 7, and 8 using the following formula: Global methylation (%) = $(1 - (\text{HpaII } \Sigma G/\Sigma T)/(\text{MspI } \Sigma G/\Sigma T)) \times 100$. Statistical analysis was performed on biological replicates using the two-tailed *t* test.

Bisulfite sequencing

Genomic DNA isolated from ES cells was bisulfite-converted using the EZ DNA Methylation-Gold kit. ICRs of three paternal and five maternal imprinted genes were amplified with two

Table 1
gRNA sequences for BAH deletion with CRISPR/Cas9

Cut site	gRNA target (intron)	gRNA sequence	Forward oligo	Reverse oligo	Genomic location	Amino acid
N terminus of BAH1	23–24	ATAAAAACCAAGCCTGATGGTGG	CACCGATAAAAACCAAGCCTGATGG	AAACCCATCAGGCTTGGTTTTTATC	9: 20919489–20919508	Ile-743
C terminus of BAH2	29–30	GCAGACGCTAGGCTAATCCTGGG	CACCGCAGACGCTAGGCTAATCCT	AAACAGGATTAGCCTAGCGTCTGC	9: 20913781–20913800	Glu-1090

Table 2
Primer sequences for bisulfite sequencing of imprinted genes (47–51)

Gene	Forward primer	Reverse primer	Genomic location	Primer source
H19	GAGTATTTAGGAGGTATAAGAATT GTAAGGAGATTATGTTTATTTTTGG	ATCAAAAACTAACATAAACCCCT CCTCATTAATCCCATAACTAT	7: 149767598; 149768017	Tremblay *et al.* (47)
Kcnq1ot1	TATAAGGAAGGTTAAGAATTTATTGTAATTATTG GTTTTTATTTTAAGTTTTTAATTTTTTATATTTGAATTT	AATTTCTTCTCTAAATCAACACRACACAAA ACAAACACTCACACCAAAAACAAAAATAAT	7: 150480959; 150481648	Hiura *et al.* (49)
Dlk1/Gtl2	AGATGTGTTGTGGATTTAGGTTGTAG AAGTGTTGTGGTTTGTTATGGGTAAG	CTAAACTACAATCTATATAATCACAACAC CCATTCCCAATCTATAAAAATATTTTAACC	12: 110766408; 110766806	Takada *et al.* (48)
Rasgrf1	GAGAGTATGTAAAGTTAGAGTTGTGTTG TAAAGATAGTTTAGATATGGAATTTTGGG	ATAATACAACAACAACAATAACAATC	9: 22824751; 22824951?	Watanabe *et al.* (51)
Peg1	GATTTGGGATATAAAAGGTTAATGAG TTTTAGATTTTGAGGGTTTTAGGTTG	TCATTAAAAACACAAACCTCCTTTAC AATCCCTTAAAAATCATCTTTCACAC	6: 30686718; 30687273	Nakamura *et al.* (50)
Peg3	TTTTTAGATTTTGTTTGGGGGTTTTTAATA TTGATAATAGTAGTTTGATTGGTAGGGTGT	AATCCCTATCACCTAAATAACATCCCTACA ATCTACAACCTTATCAATTACCCTTAAAAA	7: 6683159; 6683587	Nakamura *et al.* (50)
Snrpn	TATGTAATATGATATAGTTTAGAAATTAG AATTTGTGTGATGTTTGTAATTATTTGG	AATAAACCCAAATCTAAAATATTTTAATC ATAAAATACACTTTCACTACTAAAATCC	7: 67149878; 67150301	Hiura *et al.* (49)
Igf2r	TAGAGGATTTTAGTATAATTTTAA GAGGTTAAGGGTGAAAAGTTGTAT	CACTTTTAAACTTACCTCTCTTAC CACTTTTAAACTTACCTCTCTTAC	17: 12935002; 12935492	Hiura *et al.* (49)

rounds of nested PCR using primers listed in Table 2. The PCR product resulting from the second round of PCR was sent out for Sanger sequencing (Genewiz). Peak heights were quantified using 4Peaks software.

Immunofluorescence

ES cells were cultured on glass slides. For PCNA immunostaining, cells were treated with 0.5% Triton X-100 in CSK buffer (100 mM NaCl, 300 mM sucrose, 10 mM PIPES, pH 6.8, 3 mM $MgCl_2$, 1 mM EGTA) for 30 s at 4 °C and then treated with methanol for 20 min at −20 °C (46). Cells were permeabilized/blocked in block solution (5% donkey serum, 0.3% Triton X-100, 1× PBS) and then incubated overnight with primary antibody diluted in block solution at 4 °C. The following primary antibodies were used: mouse monoclonal to PCNA (Santa Cruz Biotechnology, sc-56 (PC10); 1:500 dilution) and rabbit polyclonal to DNMT1 (Santa Cruz Biotechnology, sc-20701; 1:500 dilution). Cells were washed 10 times with PBS and incubated for 1 h at room temperature with the following secondary antibodies diluted in block buffer: Cy2-conjugated donkey anti-mouse (Jackson ImmunoResearch Laboratories; 1:500 dilution) and IgM Alexa Fluor 594–conjugated IgG donkey anti-rabbit (Jackson ImmunoResearch Laboratories; 1:500 dilution). Slides were subsequently washed with PBS, counterstained with Hoechst 33342 (Invitrogen), and mounted with Vectorshield mounting medium (Vector Labs).

Statistical analysis

Statistical data were calculated for groups with normal distributions and similar variances. Variations within each group of data are reported as standard deviation. n represents the number of biological replicates. p values for LUMA were calculated using the two-tailed t test. The R program was used to ensure that $n = 2$ was sufficient to establish a power of 0.8. p values for bisulfite sequencing were calculated using the Mann–Whitney test.

Author contributions—O. Y., M. B., and T. H. B. conceptualization; O. Y., Z. S., N. C., and M. B. investigation; O. Y., Z. S., N. C., and M. B. visualization; O. Y., Z. S., N. C., and M. B. methodology; O. Y. and T. H. B. writing-original draft; O. Y. and T. H. B. writing-review and editing; Z. S., N. C., and M. B. validation; M. B. and T. H. B. supervision; M. B. project administration; T. H. B. funding acquisition.

Acknowledgments—We thank Lissette Delgado-Cruzada and Marius Walter for help with the LUMA assay. We thank Victor Lin and the Tom Maniatis laboratory for help with CRISPR/Cas9.

References

1. Li, E., Bestor, T. H., and Jaenisch, R. (1992) Targeted mutation of the DNA methyltransferase gene results in embryonic lethality. *Cell* **69,** 915–926 CrossRef Medline
2. Goll, M. G., and Bestor, T. H. (2005) Eukaryotic cytosine methyltransferases. *Annu. Rev. Biochem.* **74,** 481–514 CrossRef Medline
3. Edwards, J. R., Yarychkivska, O., Boulard, M., and Bestor, T. H. (2017) DNA methylation and DNA methyltransferases. *Epigenetics Chromatin* **10,** 23 CrossRef Medline
4. Yoder, J. A., Soman, N. S., Verdine, G. L., and Bestor, T. H. (1997) DNA (cytosine-5)-methyltransferases in mouse cells and tissues. Studies with a mechanism-based probe. *J. Mol. Biol.* **270,** 385–395 CrossRef Medline
5. Song, J., Rechkoblit, O., Bestor, T. H., and Patel, D. J. (2011) Structure of DNMT1-DNA complex reveals a role for autoinhibition in maintenance DNA methylation. *Science* **331,** 1036–1040 CrossRef Medline
6. Leonhardt, H., Page, A. W., Weier, H. U., and Bestor, T. H. (1992) A targeting sequence directs DNA methyltransferase to sites of DNA replication in mammalian nuclei. *Cell* **71,** 865–873 CrossRef Medline
7. Takeshita, K., Suetake, I., Yamashita, E., Suga, M., Narita, H., Nakagawa, A., and Tajima, S. (2011) Structural insight into maintenance methylation by mouse DNA methyltransferase 1 (Dnmt1). *Proc. Natl. Acad. Sci. U.S.A.* **108,** 9055–9059 CrossRef Medline
8. Bostick, M., Kim, J. K., Estève, P.-O., Clark, A., Pradhan, S., and Jacobsen, S. E. (2007) UHRF1 plays a role in maintaining DNA methylation in mammalian cells. *Science* **317,** 1760–1764 CrossRef Medline
9. Kim, J., Kim, J. H., Richards, E. J., Chung, K. M., and Woo, H. R. (2014) *Arabidopsis* VIM proteins regulate epigenetic silencing by modulating DNA methylation and histone modification in cooperation with MET1. *Mol. Plant* **7,** 1470–1485 CrossRef Medline

10. Arita, K., Ariyoshi, M., Tochio, H., Nakamura, Y., and Shirakawa, M. (2008) Recognition of hemi-methylated DNA by the SRA protein UHRF1 by a base-flipping mechanism. *Nature* **455,** 818–821 CrossRef Medline
11. Avvakumov, G. V., Walker, J. R., Xue, S., Li, Y., Duan, S., Bronner, C., Arrowsmith, C. H., and Dhe-Paganon, S. (2008) Structural basis for recognition of hemi-methylated DNA by the SRA domain of human UHRF1. *Nature* **455,** 822–825 CrossRef Medline
12. Hashimoto, H., Horton, J. R., Zhang, X., Bostick, M., Jacobsen, S. E., and Cheng, X. (2008) The SRA domain of UHRF1 flips 5-methylcytosine out of the DNA helix. *Nature* **455,** 826–829 CrossRef Medline
13. Rothbart, S. B., Krajewski, K., Nady, N., Tempel, W., Xue, S., Badeaux, A. I., Barsyte-Lovejoy, D., Martinez, J. Y., Bedford, M. T., Fuchs, S. M., Arrowsmith, C. H., and Strahl, B. D. (2012) Association of UHRF1 with methylated H3K9 directs the maintenance of DNA methylation. *Nat. Struct. Mol. Biol.* **19,** 1155–1160 CrossRef Medline
14. Liu, X., Gao, Q., Li, P., Zhao, Q., Zhang, J., Li, J., Koseki, H., and Wong, J. (2013) UHRF1 targets DNMT1 for DNA methylation through cooperative binding of hemi-methylated DNA and methylated H3K9. *Nat. Commun.* **4,** 1563 CrossRef Medline
15. Nishiyama, A., Yamaguchi, L., Sharif, J., Johmura, Y., Kawamura, T., Nakanishi, K., Shimamura, S., Arita, K., Kodama, T., Ishikawa, F., Koseki, H., and Nakanishi, M. (2013) Uhrf1-dependent H3K23 ubiquitylation couples maintenance DNA methylation and replication. *Nature* **502,** 249–253 CrossRef Medline
16. Ishiyama, S., Nishiyama, A., Saeki, Y., Moritsugu, K., Morimoto, D., Yamaguchi, L., Arai, N., Matsumura, R., Kawakami, T., Mishima, Y., Hojo, H., Shimamura, S., Ishikawa, F., Tajima, S., Tanaka, K., *et al.* (2017) Structure of the Dnmt1 reader module complexed with a unique two-mono-ubiquitin mark on histone H3 reveals the basis for DNA methylation maintenance. *Mol. Cell* **68,** 350–360.e7 CrossRef Medline
17. Li, T., Wang, L., Du, Y., Xie, S., Yang, X., Lian, F., Zhou, Z., and Qian, C. (2018) Structural and mechanistic insights into UHRF1-mediated DNMT1 activation in the maintenance DNA methylation. *Nucleic Acids Res.* **46,** 3218–3231 CrossRef Medline
18. Yang, N., and Xu, R.-M. (2013) Structure and function of the BAH domain in chromatin biology. *Crit. Rev. Biochem. Mol. Biol.* **48,** 211–221 CrossRef Medline
19. Bestor, T., Laudano, A., Mattaliano, R., and Ingram, V. (1988) Cloning and sequencing of a cDNA encoding DNA methyltransferase of mouse cells. The carboxyl-terminal domain of the mammalian enzymes is related to bacterial restriction methyltransferases. *J. Mol. Biol.* **203,** 971–983 CrossRef Medline
20. Cheng, J., Yang, H., Fang, J., Ma, L., Gong, R., Wang, P., Li, Z., and Xu, Y. (2015) Molecular mechanism for USP7-mediated DNMT1 stabilization by acetylation. *Nat. Commun.* **6,** 7023 CrossRef Medline
21. Yarychkivska, O., Tavana, O., Gu, W., and Bestor, T. H. (2018) Independent functions of DNMT1 and USP7 at replication foci. *Epigenetics Chromatin* **11,** 9 CrossRef Medline
22. Zhang, Z.-M., Liu, S., Lin, K., Luo, Y., Perry, J. J., Wang, Y., and Song, J. (2015) Crystal structure of human DNA methyltransferase 1. *J. Mol. Biol.* **427,** 2520–2531 CrossRef Medline
23. Sharif, J., Muto, M., Takebayashi, S., Suetake, I., Iwamatsu, A., Endo, T. A., Shinga, J., Mizutani-Koseki, Y., Toyoda, T., Okamura, K., Tajima, S., Mitsuya, K., Okano, M., and Koseki, H. (2007) The SRA protein Np95 mediates epigenetic inheritance by recruiting Dnmt1 to methylated DNA. *Nature* **450,** 908–912 CrossRef Medline
24. Kouzminova, E., and Selker, E. U. (2001) *dim-2* encodes a DNA methyltransferase responsible for all known cytosine methylation in *Neurospora*. *EMBO J.* **20,** 4309–4323 CrossRef Medline
25. Kim, S. C., Sprung, R., Chen, Y., Xu, Y., Ball, H., Pei, J., Cheng, T., Kho, Y., Xiao, H., Xiao, L., Grishin, N. V., White, M., Yang, X.-J., and Zhao, Y. (2006) Substrate and functional diversity of lysine acetylation revealed by a proteomics survey. *Mol. Cell* **23,** 607–618 CrossRef Medline
26. Lei, H., Oh, S. P., Okano, M., Jüttermann, R., Goss, K. A., Jaenisch, R., and Li, E. (1996) *De novo* DNA cytosine methyltransferase activities in mouse embryonic stem cells. *Development* **122,** 3195–3205 Medline
27. Damelin, M., and Bestor, T. H. (2007) Biological functions of DNA methyltransferase 1 require its methyltransferase activity. *Mol. Cell. Biol.* **27,** 3891–3899 CrossRef Medline
28. Li, E., Beard, C., Forster, A. C., Bestor, T. H., and Jaenisch, R. (1993) DNA methylation, genomic imprinting, and mammalian development. *Cold Spring Harb. Symp. Quant. Biol.* **58,** 297–305 CrossRef Medline
29. Bourc'his, D., Xu, G. L., Lin, C. S., Bollman, B., and Bestor, T. H. (2001) Dnmt3L and the establishment of maternal genomic imprints. *Science* **294,** 2536–2539 CrossRef Medline
30. Proudhon, C., Duffié, R., Ajjan, S., Cowley, M., Iranzo, J., Carbajosa, G., Saadeh, H., Holland, M. L., Oakey, R. J., Rakyan, V. K., Schulz, R., and Bourc'his, D. (2012) Protection against *de novo* methylation is instrumental in maintaining parent-of-origin methylation inherited from the gametes. *Mol. Cell* **47,** 909–920 CrossRef Medline
31. Tucker, K. L., Beard, C., Dausmann, J., Jackson-Grusby, L., Laird, P. W., Lei, H., Li, E., and Jaenisch, R. (1996) Germ-line passage is required for establishment of methylation and expression patterns of imprinted but not of nonimprinted genes. *Genes Dev.* **10,** 1008–1020 CrossRef Medline
32. McGraw, S., Zhang, J. X., Farag, M., Chan, D., Caron, M., Konermann, C., Oakes, C. C., Mohan, K. N., Plass, C., Pastinen, T., Bourque, G., Chaillet, J. R., and Trasler, J. M. (2015) Transient DNMT1 suppression reveals hidden heritable marks in the genome. *Nucleic Acids Res.* **43,** 1485–1497 CrossRef Medline
33. Bourc'his, D., and Bestor, T. H. (2004) Meiotic catastrophe and retrotransposon reactivation in male germ cells lacking Dnmt3L. *Nature* **431,** 96–99 CrossRef Medline
34. Kaneda, M., Okano, M., Hata, K., Sado, T., Tsujimoto, N., Li, E., and Sasaki, H. (2004) Essential role for *de novo* DNA methyltransferase Dnmt3a in paternal and maternal imprinting. *Nature* **429,** 900–903 CrossRef Medline
35. La Salle, S., Mertineit, C., Taketo, T., Moens, P. B., Bestor, T. H., and Trasler, J. M. (2004) Windows for sex-specific methylation marked by DNA methyltransferase expression profiles in mouse germ cells. *Dev. Biol.* **268,** 403–415 CrossRef Medline
36. Sakai, Y., Suetake, I., Itoh, K., Mizugaki, M., Tajima, S., and Yamashina, S. (2001) Expression of DNA methyltransferase (Dnmt1) in testicular germ cells during development of mouse embryo. *Cell Struct. Funct.* **26,** 685–691 CrossRef Medline
37. Bourc'his, D., and Bestor, T. H. (2006) Origins of extreme sexual dimorphism in genomic imprinting. *Cytogenet. Genome Res.* **113,** 36–40 CrossRef Medline
38. Schulz, R., Proudhon, C., Bestor, T. H., Woodfine, K., Lin, C.-S., Lin, S.-P., Prissette, M., Oakey, R. J., and Bourc'his, D. (2010) The parental non-equivalence of imprinting control regions during mammalian development and evolution. *PLoS Genet.* **6,** e1001214 CrossRef Medline
39. Holliday, R., and Pugh, J. E. (1975) DNA modification mechanisms and gene activity during development. *Science* **187,** 226–232 CrossRef Medline
40. Riggs, A. D. (1975) X inactivation, differentiation, and DNA methylation. *Cytogenet. Cell Genet.* **14,** 9–25 CrossRef Medline
41. Okano, M., Xie, S., and Li, E. (1998) Cloning and characterization of a family of novel mammalian DNA (cytosine-5) methyltransferases. *Nat. Genet.* **19,** 219–220 CrossRef Medline
42. Bewick, A. J., Vogel, K. J., Moore, A. J., and Schmitz, R. J. (2017) Evolution of DNA methylation across insects. *Mol. Biol. Evol.* **34,** 654–665 CrossRef Medline
43. Marchler-Bauer, A., Bo, Y., Han, L., He, J., Lanczycki, C. J., Lu, S., Chitsaz, F., Derbyshire, M. K., Geer, R. C., Gonzales, N. R., Gwadz, M., Hurwitz, D. I., Lu, F., Marchler, G. H., Song, J. S., *et al.* (2017) CDD/SPARCLE: functional classification of proteins via subfamily domain architectures. *Nucleic Acids Res.* **45,** D200–D203 CrossRef Medline
44. Robertson, E., Bradley, A., Kuehn, M., and Evans, M. (1986) Germ-line transmission of genes introduced into cultured pluripotential cells by retroviral vector. *Nature* **323,** 445–448 CrossRef Medline
45. Keller, G., Kennedy, M., Papayannopoulou, T., and Wiles, M. V. (1993) Hematopoietic commitment during embryonic stem cell differentiation in culture. *Mol. Cell. Biol.* **13,** 473–486 CrossRef Medline
46. Takebayashi, S., Tamura, T., Matsuoka, C., and Okano, M. (2007) Major and essential role for the DNA methylation mark in mouse embryogenesis

and stable association of DNMT1 with newly replicated regions. *Mol. Cell. Biol.* **27,** 8243–8258 CrossRef Medline

47. Tremblay, K. D., Duran, K. L., and Bartolomei, M. S. (1997) A 5′ 2-kilobase-pair region of the imprinted mouse H19 gene exhibits exclusive paternal methylation throughout development. *Mol. Cell. Biol.* **17,** 4322–4329 CrossRef Medline
48. Takada, S., Paulsen, M., Tevendale, M., Tsai, C.-E., Kelsey, G., Cattanach, B. M., and Ferguson-Smith, A. C. (2002) Epigenetic analysis of the Dlk1-Gtl2 imprinted domain on mouse chromosome 12: implications for imprinting control from comparison with Igf2-H19. *Hum. Mol. Genet.* **11,** 77–86 CrossRef Medline
49. Hiura, H., Obata, Y., Komiyama, J., Shirai, M., and Kono, T. (2006) Oocyte growth-dependent progression of maternal imprinting in mice. *Genes Cells* **11,** 353–361 CrossRef Medline
50. Nakamura, T., Arai, Y., Umehara, H., Masuhara, M., Kimura, T., Taniguchi, H., Sekimoto, T., Ikawa, M., Yoneda, Y., Okabe, M., Tanaka, S., Shiota, K., and Nakano, T. (2007) PGC7/Stella protects against DNA demethylation in early embryogenesis. *Nat. Cell Biol.* **9,** 64–71 CrossRef Medline
51. Watanabe, T., Tomizawa, S., Mitsuya, K., Totoki, Y., Yamamoto, Y., Kuramochi-Miyagawa, S., Iida, N., Hoki, Y., Murphy, P. J., Toyoda, A., Gotoh, K., Hiura, H., Arima, T., Fujiyama, A., Sado, T., *et al.* (2011) Role for piRNAs and noncoding RNA in *de novo* DNA methylation of the imprinted mouse *Rasgrf1* locus. *Science* **332,** 848–852 CrossRef Medline
52. Long, H. K., Blackledge, N. P., and Klose, R. J. (2013) ZF-CxxC domain-containing proteins, CpG islands and the chromatin connection. *Biochem. Soc. Trans.* **41,** 727–740 CrossRef Medline